PHYSICAL REVIEW A VOLUME 18, NUMBER 5 NOVEMBER 1978

Universal scaling law for K-vacancy production in heavy ion-atom single collisions

W. N. Lennard, I. V. Mitchell, and J. S. Forster
Atomic Energy of Canada Limited, Chalk River Nuclear Laboratories, Chalk River, Ontario, Canada K0J 1J0
(Received 1 June 1978)

New K-shell ionization cross sections are presented for symmetric and near-symmetric heavy-ion–atom single collisions $Z_1 \rightarrow Z_2$, with $16 \leq (Z_1, Z_2) \leq 54$ and $0.4 \leq E_1 \leq 225$ MeV. For $0.6 \lesssim Q \lesssim 1$, where $Q = Z_L/Z_H$, all data are unified by a simple scaling law, parametrized through the united-atom $2p_{1/2}$ binding energy. Existing models for K-vacancy production are shown to be inadequate.

I. INTRODUCTION

Very extensive data and detailed theories[1] have yielded powerful scaling laws describing both the total cross section and the impact-parameter dependence of K-shell ionization by fast, light, charged particles (H, He, Li, ...). However, the search for similar universal expressions to describe heavy-ion excitation systematics is in a much more primitive state, particularly for ion velocities $v_1 < v_K$ and collision pairs $Z_1 \sim Z_2$, i.e., where collisional excitation is usually described with the aid of the electron-promotion model of Fano and Lichten.[2]

Various mechanisms for K-vacancy production in heavy-ion–atom collisions have been recognized. Rotational coupling of vacancies in the $2p\pi$ molecular orbital (MO) to the $2p\sigma$ (see Fig. 1) is known to occur efficiently at small internuclear distances.[3] Further transfer via radial coupling of a $2p\sigma$ vacancy to the $1s\sigma$ MO, i.e., "K-vacancy sharing," can produce a vacancy in either collision partner.[4] For near-symmetric collision systems, $2p\pi$ and $2p\sigma$ vacancies are provided naturally by ions of all atoms having atomic numbers less than 10.

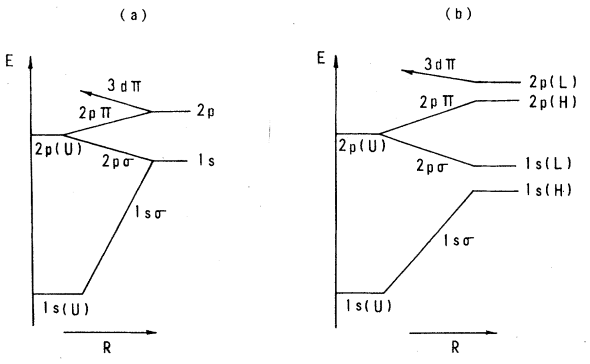

FIG. 1. Molecular-orbital correlation diagram for (a) symmetric and (b) near-symmetric collision partners. Only MO's relevant to the present discussion are shown.

For heavier ions, the atomic $2p$ shell can be opened by stripping the ion beam to charge states q such that $Z_1 - q < 10$. Short-lived $2p$ vacancies can also be performed on the projectile through ion-atom collisions in solid targets[5] and under some circumstances make the dominant contribution to the total K-vacancy cross section. The role of projectile $1s$ vacancies has also been noted.[6]

Clearly, for any target, whether gas or solid, and for whatever degree of ionization of the projectile, some part of the K-vacancy cross section can arise from mechanisms other than the above. For example, Kessel and Fastrup[7] mention two mechanisms that may contribute to K-shell ionization in near-symmetric heavy-ion–atom collisions ($Z_1, Z_2 > 10$): (i) a two-step process whereby a $2p\pi$ vacancy is performed via a long-range interaction in the *same* collision as that in which the $2p\pi$-$2p\sigma$ rotational coupling is operative; and (ii) direct (or one-step) coupling of the $2p\sigma$ MO with higher-lying vacant MO's and/or continuum states. Under single-collision conditions for which the $2p$ exit channels are closed, we may expect such mechansims to make a major contribution to the total K-ionization cross section. Saris *et al.*[8] and Winters *et al.*[9] both suggested that the second mechanism dominates in gas-target K-shell ionization where $14 \leq Z_1, Z_2 \leq 18$. In conflict with this viewpoint, Cocke *et al.*[10] reported a signature characteristic of $2p\pi$-$2p\sigma$ rotational coupling in their 15- and 30-MeV Cl→Ar impact-parameter data. In a recent summary of $2p$ excitation, Meyerhof *et al.*[11] have concluded that the importance of the one-step process cannot be ascertained without further work. The situation is not clarified by the recent results of Lutz *et al.*[12] who reported that the impact-parameter dependence of K-vacancy production in Ar-Ar single collisions, $2.5 < E < 8.0$ MeV, cannot be explained by any current theoretical model.

Even without clear evidence for specific K-excitation mechanisms, several authors have sought universal expressions for K-vacancy-production

cross sections in heavy-ion–atom collisions. Meyerhof *et al.*[11] attempted to describe K-shell ionization for *symmetric* collision pairs ($Z_1 = Z_2$) by parametrizing the cross sections through the united atom ($Z^{UA} = 2Z_1$) $2p$-shell binding energy. At that time, there was a dearth of single-collision data. This initiative was followed by Foster *et al.*[13] who tried to describe single-collision cross sections for symmetric *and* near-symmetric collision systems through a modification of the binary encounter approximation.[1] Nevertheless, they relied heavily on solid-target data. Brandt *et al.*[14] also made no distinction between single-collision and solid-target data when comparing experimental results with predictions of a vacancy-diffusion model of K-shell excitation. As indicated above, a failure to separate gas- from solid-target data can obscure the differences between $2p$-vacancy assisted (exit channel open) and unassisted (exit channel closed) situations.

In large measure, the difficulty of constructing models and scaling relationships for K-excitation in heavy-ion–atom single collisions is attributable to a sparseness of cross-section and impact-parameter data. For the same reason(s), it is not easy to estimate single-collision excitation contributions in solid-target (e.g., thin films) experiments.[15] Cross-section values are also needed to normalize relative ionization probabilities to absolute values.[12]

To help provide a broader data base, we have undertaken measurements of single-collision K-shell ionization cross sections, with emphasis on collision systems heavier than most of those studied thus far. In this paper, we present new cross-section data taken with gaseous targets and *closed* $2p$-shell electron configurations for the projectiles. The experimental method is outlined in Sec. II. In Sec. III, we present the results of measurements made for both symmetric and near-symmetric systems in the range $16 \leq Z_1, Z_2 \leq 54$.

We show that all of our cross-section data are embraced by an empirical scaling law provided $0.6 \lesssim Q \leq 1.0$, where $Q = Z_L / Z_H$ (Z_L being the lower Z, Z_H being the higher Z). These measurements establish, incidentally, that $\sigma_K(Z_L \rightarrow Z_H) \equiv \sigma(Z_H \rightarrow Z_L)$, an equality that is *not* preserved for asymmetric systems where the projectile carries preformed $2p$ vacancies (e.g., when the projectile is highly stripped or traverses solid targets). We compare our results with all other available single-collision K-excitation data and conclude that all are expressible by the same empirical scaling law.

In Sec. IV, we examine recent attempts to find a scaling relationship for K-vacancy cross sections and show that some are quite unable to describe the data. It is also apparent that existing impact-parameter measurements do not lead to a unique description of K-vacancy production by heavy ions.

II. EXPERIMENT

Beams of ^{1}H, ^{32}S, ^{35}Cl, ^{58}Ni, ^{63}Cu, ^{74}Ge, ^{75}As, ^{80}Se, ^{79}Br, and ^{127}I ions were obtained from the Chalk River Nuclear Laboratories 13-MV MP tandem accelerator, and of ^{1}H, ^{40}Ar, and ^{55}Mn ions from the Chalk River Nuclear Laboratories 2-MV high-voltage mass separator (HVMS). Table I lists the systems studied.

TABLE I. Near-symmetric and symmetric collision systems and energy regions for which total K x-ray cross sections have been measured under single-collision conditions, i.e., using gas targets. The last column gives the minimum $t^{1/2}$ values (see the Appendix for discussion) corresponding to a laboratory detector angle $\phi = 44°$.

Collision system	Energy region (MeV)	$t^{1/2}$ (minimum)
$^{32}S \rightarrow Ar$	10 – 30	108
$^{35}Cl \rightarrow Ar$	10 – 30	101
$^{40}Ar \rightarrow Ar$	0.4– 2.5	3.77
$^{55}Mn \rightarrow Ar$	1.3– 2.0	7.25
$^{63}Cu \rightarrow Ar$	12 – 50	51.8
$^{58}Ni \rightarrow Kr$	20 – 80	50.5
$^{63}Cu \rightarrow Kr$	20 – 80	48.3
$^{74}Ge \rightarrow Kr$	20 – 80	42.9
$^{75}As \rightarrow Kr$	20 – 80	41.4
$^{80}Se \rightarrow Kr$	20 – 80	39.9
$^{79}Br \rightarrow Kr$	8 –100	15.4
$^{127}I \rightarrow Kr$	42 –149	41.0
$^{79}Br \rightarrow Xe$	26 – 59	31.6
$^{127}I \rightarrow Xe$	42 –225	31.1

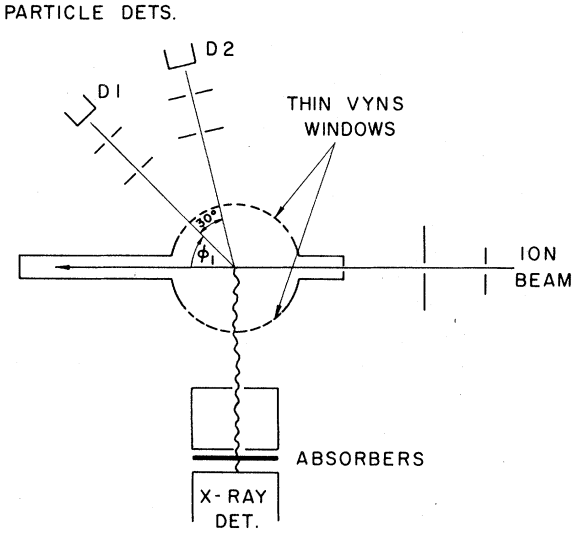

FIG. 2. Schematic gas cell arrangement used for heavy-ion-induced x-ray cross-section measurements on the MP tandem accelerator. $D1$ and $D2$ are surface barrier detectors.

The ion beams were directed into differentially pumped gas cells containing high-purity Ar, Kr, or Xe gas. The 5-cm-diam gas cell used for the tandem experiments is shown schematically in Fig. 2. Gas pressure in the cell was monitored by a calibrated thermocouple gauge and was maintained at values in the range 10(Ar) – 150(Kr, Xe) mTorr (1.3–20 Pa). X-rays and particles escaped into a large, concentric vacuum chamber through windows of approximately 50-μg cm^{-2} VYNS supported on 0.005-mm nickel mesh. The geometric transmission of the mesh was measured to be 58%. Two surface-barrier particle detectors $D1$ and $D2$ were located in the large chamber at laboratory scattering angles $\phi_1 = 44°$ and $\phi_2 = \phi_1 + 30°$, respectively. Each was collimated by a pair of identical Ta apertures with slit widths of 1 or 2 mm, resulting in $\Delta\phi$ of $\pm 3°$ or $\pm 6°$. The gas-target length viewed by $D1$ at $\phi = 44°$ was 0.75 cm for a slit width of 1 mm, corresponding to a target thickness of 0.04 μg cm^{-2} for 1.3 Pa of Kr.

The target cell used for the HVMS experiment was a double differentially pumped cell of simpler design[16] and having only one particle detector, fixed at $\phi = 44.5°$ and mounted in the target gas ambient. The cell pressure was monitored with a capacitance manometer and maintained at ~10 mTorr.

Within statistics, all K x-ray cross sections were unchanged by fourfold pressure reductions in both target-gas cells and we conclude that the gas targets provided single-collision conditions for *K-vacancy excitation* (of course these do not necessarily provide single-collision conditions for L-shell, M-shell... ionization measurements).

Si(Li) and intrinsic Ge x-ray detectors were used, the choice depending on the energy and intensity of the x rays to be detected. Only relative detection efficiencies were measured for these detectors, since absolute efficiencies were not required in the data reduction. These detectors were always located at 90° to the beam and were collimated to view approximately the same gas volume as seen by the particle detectors. Suitable Al or Be absorbers were used to attenuate unwanted low-energy photons.

All heavy-ion measurements were complemented by proton measurements taken in identical geometry. By counting scattered particles, we obviated the need for current integration, for absolute gas-pressure measurements and for measurement of absolute detector geometries. The total K-ionization cross section σ_K for heavy-ion bombardment $Z_1 \rightarrow Z_2$ is $\sigma_K = \sigma_K(1) + \sigma_K(2)$ and may be evaluated from the expression

$$\sigma_K = \frac{\sigma_p}{\sigma_p^0} \frac{N_p^0}{N_p} \frac{\sigma_K^0}{Y_2^0} \left(Y_2 + \frac{\epsilon_2}{\epsilon_1} \frac{\omega_2}{\omega_1} \frac{A_1}{A_2} \frac{C_1}{C_2} Y_1 \right), \tag{1}$$

where σ_p is the elastic-scattering cross section in the laboratory frame (including recoils) for $Z_1 \rightarrow Z_2$ to laboratory angle ϕ; $\sigma_p^0 = \sigma_p$ for $^1\mathrm{H} \rightarrow Z_2$ at angle ϕ (no recoils); N_p is the scattered projectile plus recoil target atom yield; N_p^0 is the scattered proton yield; σ_K^0 is the proton-induced K-ionization cross section (see Table II for adopted values); Y_2^0 is the target-gas $K\alpha$ x-ray yield for proton excitation; Y_1 and Y_2 are the projectile and target $K\alpha$ x-ray yields for $Z_1 \rightarrow Z_2$; ϵ_1 and ϵ_2 are the x-ray detector efficiencies for $K\alpha$ x rays from Z_1 and Z_2; ω_1 and ω_2 are the neutral-atom K-shell fluorescence yields[17]; A_1 and A_2 are the absorption of $K\alpha$ x-rays emitted by Z_1 and Z_2; and $C_1, C_2 = (1 + K_\beta/K\alpha)$ for Z_1, Z_2.[17] In almost all cases, values of σ_p and σ_p^0 are obtained from the Rutherford formula (see the Appendix). Isotropic K

TABLE II. Values of proton-induced K-ionization cross sections (σ_K^0) used to normalize heavy-ion-induced x-ray yields from gas targets. Bracketed quantities indicate powers of 10.

System	σ_K^0 (cm^2)	Reference
0.5-MeV ^{1}H → Ar	2.45 (−22)	46
1.0-MeV ^{1}H → Kr	1.63 (−24)	47
3.0-MeV ^{1}H → Ar	4.80 (−21)	48, 49, 52
3.0-MeV ^{1}H → Kr	3.06 (−23)	48, 49
3.0-MeV ^{1}H → Xe	4.81 (−25)	48, 49

x-ray emission is also assumed. For $Z>20$, the use of neutral-atom fluorescence yields is expected to be reliable since $\omega_K>0.15$. For S, Cl, and Ar ($16\leq Z_1, Z_2\leq 18$), additional uncertainties arise, as discussed later.

We have measured the Br→Kr and Cu→Kr cross sections at 55 MeV on several occasions, using different x-ray detectors and slightly different particle and x-ray geometries, but normalizing always via the ^{1}H→Kr K x-ray cross section at 3 MeV. Reproducibility was better than 6% in all cases.

We have been careful to use beams Z_1^{q+} with q restricted to values that ensured the projectile $2p$ shell was completely full, i.e., $Z_1-q\geq 10$. The K x-ray cross section for 78.5-MeV $^{79}Br^{q+}$→Kr varied by less than 2% per charge-state increment for $7\leq q\leq 20$. The effect of deliberately stripping into the $2p$ shell was also examined and is discussed later. (The high charge state Br^{q+} beams were produced by postacceleration stripping in carbon foils.)

We have also checked for possible x-ray yields from internal conversion decay of Coulomb-excited nuclear states. In all cases, this process contributes negligibly to the total K x-ray cross sections we have measured.

The uncertainties in the absolute K-ionization cross section values are the following.

(a) The systematic uncertainties in the values used for proton excitation (as shown in Table II) are estimated to be 10%.

(b) The uncertainties due to the curve fitting used in extracting x-ray and particle yields are 0.5%–3%, including statistical errors.

(c) For heavy-ion–atom collisions, $K_\beta/K\alpha$ ratios are found to be consistently lower than those observed for fluorescence.[17] This is attributed to a reduction of the K_β intensity as a consequence of multiple M-shell ionization.[18] We have therefore used only the $K\alpha$ yields and neutral atom K_β/K_α values to extract K-shell ionization cross sections. This procedure introduces a maximum uncertainty of 4%.

(d) For systems where $Z_1, Z_2>20$, the uncertainty in the ω_K values is estimated to be <10%. For lighter target-projectile systems, an uncertainty of 40% is arbitrarily allowed.[10]

(e) The uncertainty in determining the particle scattering angle, including the effect of the finite solid angle, is <1%. This estimate includes the uncertainty in the elastic-scattering cross sections used (see the Appendix) except in a few cases (e.g., Ar→Ar at 1 MeV or lower) where it may be as large as 5%.

(f) The absorption due to the use of x-ray filters to remove low-energy photons introduces an uncertainty <1%.

(g) The error in the relative detection efficiencies for x rays is less than 5%.

(h) No error has been included for x-ray anisotropy. Published data[19,20] indicate angular distributions are isotropic.

Thus the typical experimental uncertainty (i.e., $Z_1, Z_2>20$) is approximately 13%, plus the systematic 10% uncertainty contained in the proton-induced cross-section normalization.

We note, finally, that the data analysis is direct, involving none of the corrections for energy loss, recoil, or straggling effects that are required for solid-target data.[21]

III. RESULTS

A. New data

To within 15%, the K-vacancy cross sections were found to be distributed between asymmetric collision partners $Z_L, Z_H\geq 25$ according to the Meyerhof formula[4] for $2p\sigma$-$1s\sigma$ radial coupling:

$$\sigma_K(H)/\sigma_K(L)=\exp(-2X_K)\,, \tag{2}$$

where $X_K=13.46\{[I_{1s}(H)]^{1/2}-[I_{1s}(L)]^{1/2}\}v_1$. Here $I_{1s}(H,L)$ is the atomic K-electron binding energy in keV for neutral atoms (Z_H, Z_L) and v_1 is the projectile velocity in a.u. This result is consistent with the experimental boundary conditions: (i) $Q\gtrsim 0.6$, which has the effect of suppressing K-L level matching contributions[22]; and (ii) $v/v_K<1$, i.e., where direct $1s\sigma$ excitation is weak. For the two cases S, Cl→Ar, discrepancies up to 40% appear. Such effects have been noted before[9] and have been associated with fluorescence-yield changes.

Values for the total K-vacancy cross sections σ_K i.e., summed over both collision partners, are listed in Table III. The data span the region $16\leq Z_1, Z_2\leq 54$ for projectile energies $0.4\leq E(Z_1)\leq 225$ MeV (see Table II). They may be displayed conveniently[11,13] as scaled cross sections $[I_{2p}(U)/Z]^2\sigma_K$ plotted against the scaling parameter

$$[v_1/v_{2p}(U)]^2=(E_1/M_1)/[I_{2p}(U)/m_e]\,.$$

Here, $I_{2p}(U)$ is the *united atom* ($Z^{UA}=Z_1+Z_2$) $2p_{1/2}$ binding energy in keV and Z is the effective charge, $2Z^2=Z_1^2+Z_2^2$. σ_K is the K-ionization cross section in cm^2, M_1 and m_e are the projectile and electron masses, respectively, and E_1 is the projectile energy. We have used the tables of Fricke and Soff[23] to obtain the united-atom $2p_{1/2}$ binding energies for the I-Xe system ($Z^{UA}=107$); otherwise the values are taken from the tables of Bearden.[24]

The results are shown in Fig. 3. Over almost six decades the scaling produces a remarkable uni-

TABLE III. Summary of K-shell ionization cross sections for $Z_1^{q+} \rightarrow Z_2$ at energy E_1, summed over both collision partners. Bracketed quantities indicate powers of 10.

Projectile	Target	q	E_1 (MeV)	σ_K (cm^2)
^{40}Ar	Ar	1	0.4	1.3 (−24)
		1	0.5	5.7 (−24)
		1	0.61	1.7 (−23)
		1	0.8	5.3 (−23)
		1	1.0	1.6 (−22)
		1	1.5	3.7 (−22)
		1	2.0	7.9 (−22)
		2	2.5	1.3 (−21)
^{55}Mn	Ar	1	1.3	1.4 (−24)
		1	2.0	2.6 (−23)
^{32}S	Ar	3	10	7.6 (−20)
		4	20	3.2 (−19)
		4	30	4.9 (−19)
^{35}Cl	Ar	3	10	5.0 (−20)
		4	20	1.9 (−19)
		4	30	3.7 (−19)
^{63}Cu	Ar	4	12	1.9 (−21)
		4	25	1.3 (−20)
		6	50	5.2 (−20)
^{58}Ni	Kr	4	20	2.7 (−22)
		5	40	2.0 (−21)
		6	55	4.7 (−21)
		7	80	9.0 (−21)
^{63}Cu	Kr	4	20	1.7 (−22)
		5	40	1.3 (−21)
		6	55	3.2 (−21)
		7	80	6.9 (−21)
^{74}Ge	Kr	4	20	8.4 (−23)
		5	40	5.8 (−22)
		6	55	1.2 (−21)
		7	80	4.0 (−21)
^{75}As	Kr	4	20	5.8 (−23)
		5	40	4.5 (−22)
		6	55	1.2 (−21)
		7	80	2.8 (−21)
^{80}Se	Kr	4	20	3.1 (−23)
		5	40	2.2 (−22)
		6	60	5.9 (−22)
		7	80	2.6 (−21)
^{79}Br	Kr	4	8	8.5 (−25)
		4	10	3.2 (−24)
		4	20	2.8 (−23)
		5	40	2.9 (−22)
		6	55	8.4 (−22)
		7	80	2.1 (−21)
		8	100	3.9 (−21)
^{127}I	Kr	6	42	3.1 (−24)
		9	94	7.3 (−23)
		16	149	2.5 (−22)
^{79}Br	Xe	5	26	3.4 (−24)
		7	59	8.5 (−23)
^{127}I	Xe	6	42	3.1 (−25)
		9	94	5.7 (−24)
		16	149	1.7 (−23)
		21	225	8.2 (−23)

fication of all of our data, for both symmetric *and* asymmetric collision systems, provided $Q = Z_L/Z_H \gtrsim 0.6$. The minimum value of Q included here is $Q = 0.621$ for the Cu-Ar system. (In those cases where $Q < 0.6$, the cross sections are discordant, signaling a different excitation process, see Sec. III E.)

All of the cross-section data are well described by a polynomial (shown by the solid curve) of the form

$$f(y) = \sum_{i=1}^{5} a_i y^{i-1} \tag{3}$$

with $a_1 = -20.665$, $a_2 = -1.332$, $a_3 = -2.276$, $a_4 = -0.482$, and $a_5 = -0.0469$. Here, $y = \log_{10} \times \{[v_1/v_{2p}(U)]^2\}$ and $f(y) = \log_{10}\{[I_{2p}(U)/Z]^2 \sigma_K\}$. The scatter is small but generally greatest for the lightest collision systems, $16 \leq Z_1, Z_2 \leq 18$, i.e., where uncertainties in fluorescence yield values are largest. Expression (3) fits two-thirds of the data to within 25%, and essentially *all* the data to within a factor of 2. The dashed curve in Fig. 3 represents the modified BEA prescription[13] and is discussed in Sec. IV.

B. Comparison with other data

We show in Fig. 4 all available single-collision data ($v_1/v_K < 1$, $0.6 \lesssim Q \leq 1.0$), both published and communicated privately, plotted as in Fig. 3. For the sake of clarity, our data are represented by the empirical scaling curve, expression (3) reproduced from Fig. 3. The agreement between our data and all other data is satisfactory. A specific example is provided by the Cl → Ar data. The K-ionization cross sections measured by the Kansas

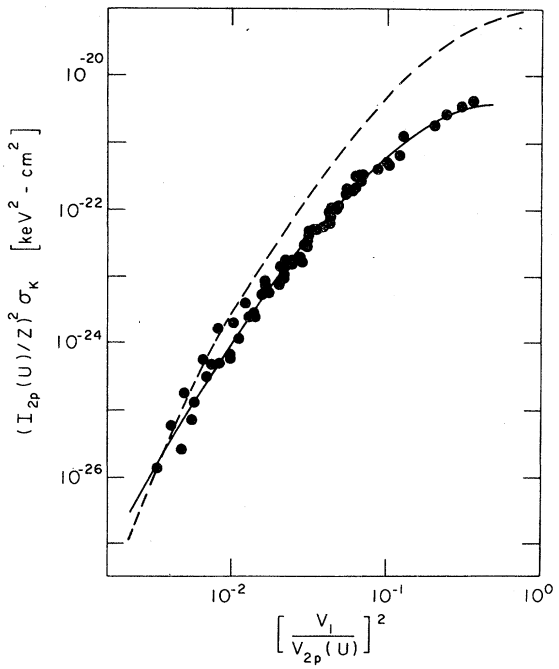

FIG. 3. Scaled single-collision K-vacancy cross sections for symmetric and near-symmetric ($0.6 \lesssim Q \leq 1.0$) collision systems. The cross-section values are given in Table III. The scaling parameters are given in the text. The solid curve represents a polynomial fit to the data [see expression (3) in text]. The dashed curve is the modified BEA proposal of Ref. 13.

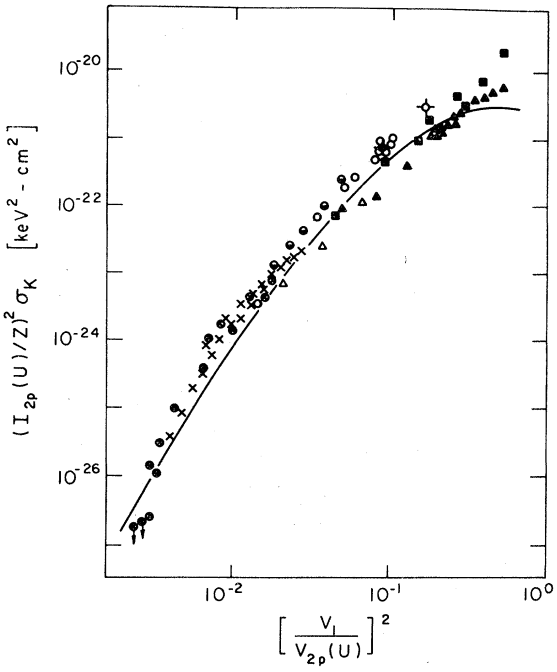

FIG. 4. Same as Fig. 3 except the data are from other sources: (⊗) Ref. 8; Ar→Ar, Ar→Cl; (✦) Ref. 28; Cu→Kr; (▲) Ref. 9; Cl→Si, Cl→S, Cl→Cl, Cl→Ar, S→Si, S→S, S→Cl, S→Ar; (■) Ref. 25; Cl→Ar; (○) Ref. 11; Kr→Kr, Xe→Xe, Xe→Kr; (✕) Ref. 51; Ar→Ar, Ar→Si; (□) Ref. 10; Cl→Ar; (◇) Ref. 50; Al→Ar. The smooth curve is our empirical scaling result from Fig. 3.

group,[9] the Heidelberg group,[25] and by us, are shown in Fig. 5 for $4 \leq E_1 \leq 52.5$ MeV. Since different errors can arise from different sources in these measurements (e.g., in the proton ionization cross sections we adopted, in the x-ray detector efficiencies and detector geometries used), the accord is considered good. It will be noted that although the cross-section data of other groups span an equally wide range of scaled velocities, $[v_1/v_{2p}(U)]^2$, the variety of collision partners is much more limited than that shown in Fig. 3.

Together the data bases establish confidence that in near-symmetric and symmetric heavy-ion collisions there is a smooth variation of scaled cross section versus scaled velocity. The significance of this result is discussed in Sec. IV.

C. Reciprocity

We have measured values for $\sigma_K(Z_1 \rightarrow Z_2)$ and $\sigma_K(Z_2 \rightarrow Z_1)$ for the systems Br→Xe and I→Kr at two velocities. For these pairs Q takes similar values (0.648 and 0.679, respectively), and $Z^{UA} = Z_1 + Z_2 = 89$ for both. In each comparison, beam

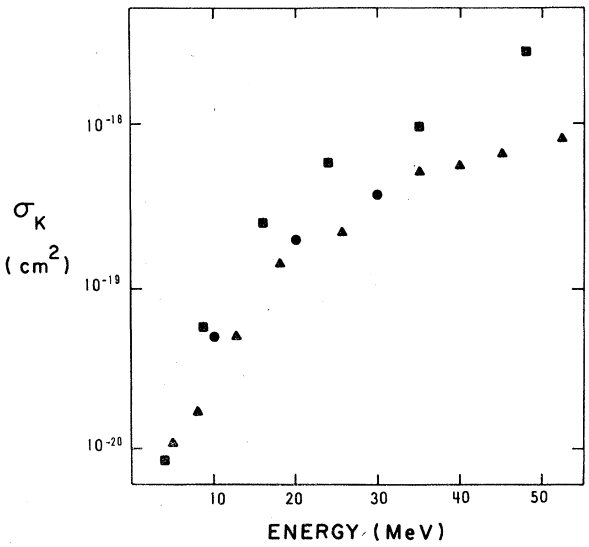

FIG. 5. K-ionization cross sections for Cl→Ar collisions as a function of projectile energy E_1. Neutral-atom fluorescence yields have been used to convert measured x-ray cross sections to K-vacancy cross sections. (●) this work; (▲) Ref. 9; (■) Ref. 25.

TABLE IV. Total K-ionization cross sections for the complementary collision pairs, Br → Xe and I → Kr, at the same velocity. Bracketed quantities indicate powers of 10.

Collision system	Projectile velocity (MeV/amu)	σ_K (cm^2)
$^{79}Br \rightarrow Xe$	0.329	3.4 ± 0.6 (−24)
$^{127}I \rightarrow Kr$	0.331	3.1 ± 0.5 (−24)
$^{79}Br \rightarrow Xe$	0.747	8.5 ± 1.4 (−23)
$^{127}I \rightarrow Kr$	0.740	7.3 ± 1.2 (−23)

energies were chosen to keep the relative velocities the same. The charge states of the beams never exceeded $q = 9$, well below the value at which the $2p$ shell is opened. Since $\omega_K > 0.6$, reliable values for the ionization cross sections can be obtained from the x-ray cross sections. The results are shown in Table IV and within the errors (17%), confirm the identity $\sigma_K(Z_1 \rightarrow Z_2)$. The same reversibility is to be found in the near-symmetric gas-target data of Winters *et al.*,[9] representing a much-lower-Z system. Using neutral-atom fluorescence yields, we obtain $\sigma_K = 2.2 \times 10^{19}$ cm^2 and 2.4×10^{19} cm^2 for $S^{5+} \rightarrow HCl$ and $Cl^{5+} \rightarrow H_2S$, respectively, at a common velocity of 0.51 MeV/amu. Such equalities would *not* be expected if (constant velocity) cross sections were compared for $Z_1(2p^{-1}) \rightarrow Z_2$ and $Z_2(2p^{-1}) \rightarrow Z_1$, for example, due to the unequal partition of $2p$ vacancies between the radially coupled $3d\pi$ and $2p\pi$ molecular orbitals,[26] which correlate to the $2p(L)$ and $2p(H)$ separated-atom orbitals, respectively [see Fig. 1(b)].

D. Projectile charge-state effects

We deliberately chose collision partners whose atomic $2p$ shells were full prior to the collision. Without this precaution, vacancies could be introduced into the $2p\pi$ orbital (or couple into the $2p\pi$ radially from the $3d\pi$ orbital) and then obscure processes (i) and (ii). Observing the constraint that the $2p$ shell carry no vacancies into the collision, we have searched for a dependence of the K x-ray cross section upon projectile charge state q. We found no evidence for such a dependence of σ_x upon q in any of the data 20–80-MeV $Z_1^{q+} \rightarrow Kr$, $Z_1 = 28$, 29, 32, 33, 34, and 35 and with q taking values $3 \leq q \leq 8$. The results of a more detailed investigation for 78.5-MeV Br^{q+} collisions with Kr, $7 \leq q \leq 20$, i.e., with projectile electron number Z_1-q ranging between 28 and 15, are shown in Fig. 6. The x-ray cross section changes by less than

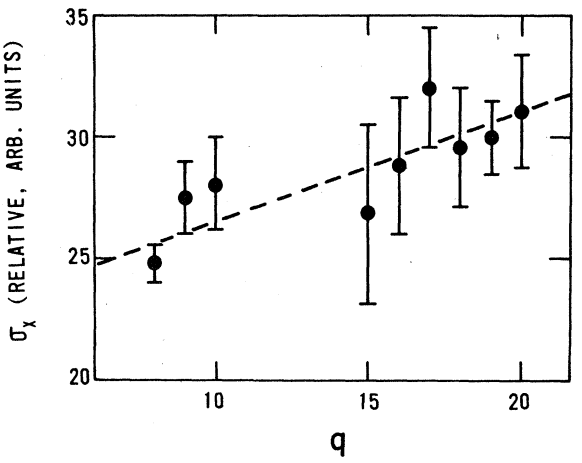

FIG. 6. Relative K x-ray cross sections for 78.5-MeV $^{79}Br^{q+} \rightarrow Kr$ as a function of the projectile charge state q. The dashed line is the best linear fit to the data. Note the suppressed zero on the ordinate scale.

2% per charge state over this region. A similar constancy has been reported by Schiebel *et al.*[27] for 66-MeV $Cu^{q+} \rightarrow Ar$ ($10 \leq q \leq 19$) and by Warczak *et al.*[28] for 88.2-MeV $Cu^{q+} \rightarrow Kr$ ($16 \leq q \leq 19$). These data are reproduced in Figs. 7 and 8, respectively. Even for low-Z collision pairs, where significant changes in K-shell fluorescence yields can be expected as the electron number is depleted, the K x-ray cross sections are rather insensitive to projectile charge state, so long as the $2p$ shells are full. Our own data for 30-MeV $S^{q+} \rightarrow Ar$ and the

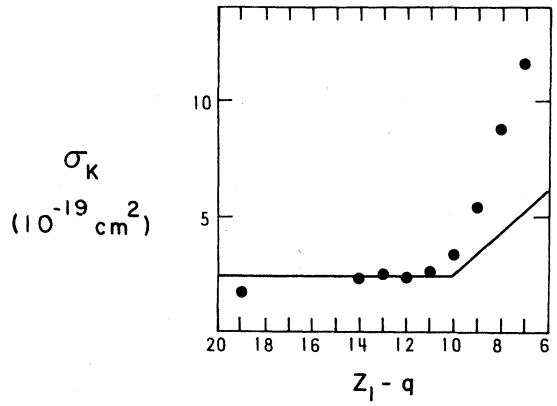

FIG. 7. K-ionization cross section for 66-MeV $^{63}Cu^{q+} \rightarrow Ar$ as a function of projectile electron number $Z_1 - q$ taken from Ref. 27. The solid line is constructed by assuming σ_K is a constant for $Z_1 - q \geq 10$ and, for $Z_1 - q < 10$, by superposing the $2p\pi$-$2p\sigma$ rotational coupling contribution calculated for each additional $2p$ vacancy as described in the text.

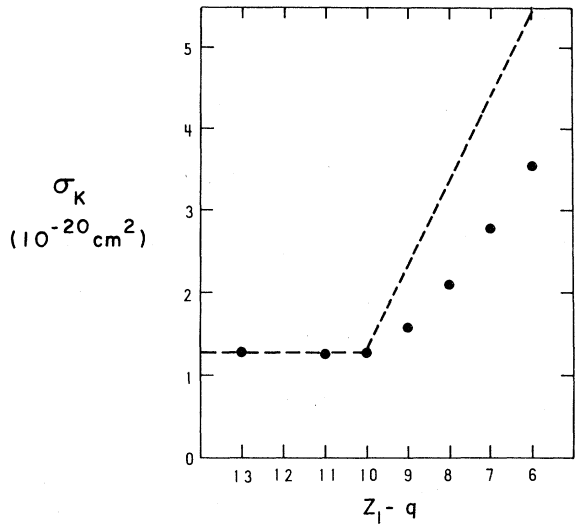

FIG. 8. Same as Fig. 7 but for 88.2-MeV $^{63}Cu^{q+} \rightarrow Kr$, taken from Ref. 28. The dashed curve is a calculation (see text).

data of Winters *et al.*[9] for 18-MeV $Cl^{q+} \rightarrow Ar$ and 18-MeV $Cl^{q+} \rightarrow H_2S$ are shown in Fig. 9. We conclude that the degree of ionization of the projectile does *not* affect the total K-shell ionization cross section, so long as $Z_1 - q \geq 10$.

The situation changes dramatically as the $2p$ shell is opened ($Z_1 - q < 10$). This represents the open-exit-channel case[7] and for each additional $2p$ vacancy, a corresponding increase in the total K x-ray cross section is observed (Figs. 7–9). For S → Ar, Cl → Ar, and Cu → Kr, the $2p$ vacancy on the projectile correlates to the $3d\pi$ orbital and is radially coupled[26] to the $2p\pi$ orbital with a coupling probability

$$W_L = [1 + \exp(1.79 X_L)]^{-1} , \qquad (4)$$

where $X_L = 13.46 \{[I_{2p}(H)]^{1/2} - [I_{2p}(L)]^{1/2}\}/v_1$. Here, $I_{2p}(H, L)$ are the separated-neutral-atom $2p$ binding energies for Z_H, Z_L in keV, and v_1 is the projectile velocity in a.u. For Cl → S and Cu → Ar, the projectile $2p$ shell correlates to the $2p\pi$ molecular orbital but the same $3d\pi$-$2p\pi$ radial coupling will operate to reduce the fraction of $2p\pi$ MO vacancies. A straightforward calculation using σ_{rot}, where σ_{rot} is the $2p\pi$-$2p\sigma$ rotational coupling cross section, then leads to a K-ionization cross-section contribution, $\Delta\sigma_K$ per $2p$ vacancy, i.e., we assume that $\Delta\sigma_K \alpha n$, where n is the number of $2p$ vacancies on the projectile. (There is experimental evidence[29] from $Ne^{q+} \rightarrow Ne$ K-ionization data that this assumption is reasonable.) These calculated values are plotted in Figs. 7–9, superposed on the experimental mean cross section measured for $Z_1 - q \geq 10$, i.e., $n = 0$. In view of the assumption

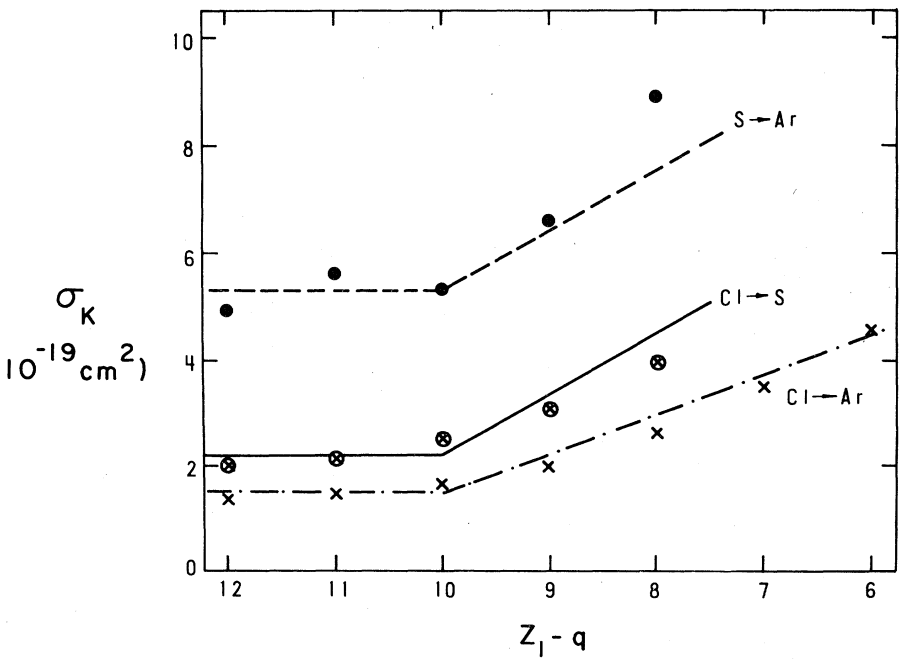

FIG. 9. Same as Fig. 7 for (●---●) 30-MeV $^{32}S^{q+} \rightarrow Ar$; (×--·-×) 18-MeV $^{35}Cl^{q+} \rightarrow Ar$, from Ref. 9; (⊗—⊗) 18-MeV $^{35}Cl^{q+} \rightarrow H_2S$, from Ref. 9. The smooth curve is a calculation (see text).

contained in this calculation, viz., that σ_{rot} is independent of q and also that no allowance has been made for any dependence of ω_K upon q, the agreement between calculated values and experiment is good. It is interesting to note that the electron yields measured by Cocke et al.[10] for 30-MeV $Cl^{q+} \rightarrow Ar$ ($q = 6$, 10, 11) show no dependence upon charge state, an anomaly that might be reconciled by associating a shrinking Auger yield with increasing q.

E. K-L level matching

Our interest in single-collision data relates to collision systems with values of $Q \gtrsim 0.6$ and therefore sufficiently near to symmetry that $2p\sigma$ excitation dominates.[11] In the course of our work, however, we have made K x-ray measurements for more asymmetric collisions, S, $Cl \rightarrow Kr$ ($Q = 0.444$, 0.472), and $Br \rightarrow Ar$ ($Q = 0.514$). The gas-target σ_K values obtained may be compared with those measured by Winters *et al.*[9] for S, $Cl \rightarrow Kr$ and $S \rightarrow Br$ systems. [Note that $\sigma_K(H) \ll \sigma_K(L)$ for all of these collision systems.] Where direct comparisons can be made, the agreement is excellent, generally within 30%. Figure 10 shows all these $Q \sim 0.5$ data, including the data of Warczak *et al.*[28] for 88.2-MeV $Cu \rightarrow Xe$ ($Q = 0.537$). The solid line represents our near-symmetric scaling result of Fig. 3. It is evident that our scaling relation is inappropriate for these more asymmetric systems.

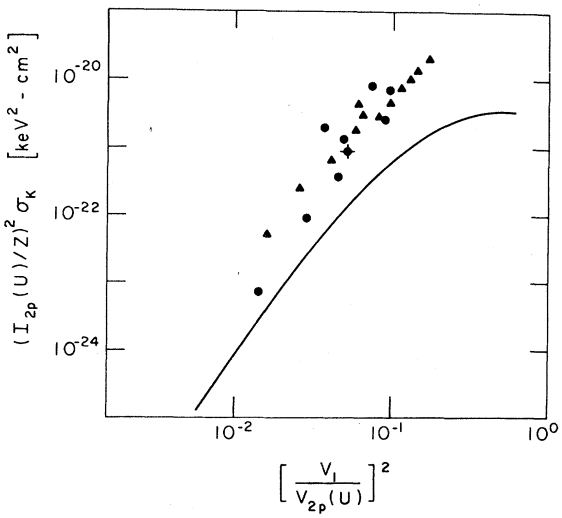

FIG. 10. Scaled K-vacancy single-collision cross sections for a variety of collision systems, $Q \sim 0.5$. The data are plotted as in Fig. 3. (●) this work, (▲) Ref. 9, (◆) Ref. 28. The smooth curve is empirical scaling result of Fig. 3 for $Q \gtrsim 0.6$ systems.

For hydrogenic energy levels, the condition $Q = 0.5$ leads directly to equal atomic binding energies, $I(n=2, Z_H) = I(n=1, Z_L)$, i.e., K-L level matching. In this region, Meyerhof *et al.*[22] have shown that K-L level matching contributions dominate K-vacancy production; evidence was drawn from data for Ni, Br, and I beams bombarding solid targets, $Q = 0.40$–0.45. In the K-L level matching scheme, Meyerhof *et al.*[22] proposed that vacancies initially formed in the $3d\sigma$ MO are shared between the collision partners on the outgoing part of the collision, i.e., between $1s(L)$ $2s(H)$, $2p(H)$, leading to an enhancement in the Z_L K-ionization cross section. Until a more quantitative account of $3d\sigma$ excitation is available, it is not easy to gauge the importance of K-L level matching effects in single-collision K cross sections for the region $Q \gtrsim 0.6$ and we do not consider them further here.

IV. DISCUSSION

We restrict our attention to those single-collision K-shell ionization processes characterized by $v_1 < v_K$ and $0.6 \lesssim Q \leq 1.0$. These boundary conditions are equivalent, respectively, to a suppression of $\sigma_{1s\sigma}$ excitation and of the K-L level matching mechanisms (which can lead to $2p\sigma$ vacancies).[21] A measurement of σ_K thus constitutes a measurement of $\sigma_{2p\sigma}$ and the mechanisms of interest are consequently those that can ionize the $2p\sigma$ MO directly, and those that ionize the $2p\pi$ MO, which may then couple rotationally to the $2p\sigma$ MO, i.e., mechanisms (i) and (ii).

Meyerhof *et al.*[30] were the first to note that the very few single-collision ($Z > 10$) K-excitation cross sections then available were unified in some fashion by parametrizing the velocity dependence through the binding energy $G(D)$ of the $2p\sigma$ MO, evaluated at the distance of closest approach D. No attempt was made to simultaneously accommodate symmetric and asymmetric collision data. Although they drew upon some solid-target data, Meyerhof *et al.*[30] pointed out that only gas-target data should be admitted. No theory of $2p\sigma$ ionization emerged from this study.

Foster *et al.*[13] also considered the effect of modified binding energies upon K-ionization cross sections, following a suggestion by Hansen.[31] They simulated it by using united-atom (UA) $2p$ binding energies instead of the separated-atom (SA) $1s$ binding energies in a BEA model of direct excitation. This prescription does not reproduce either the absolute magnitude or the energy dependence of our data very well, as may be judged from Fig. 3. The earlier apparent agreement between prediction and experiment is largely des-

troyed if one removes from the comparison the *solid*-target cross-section data of Kubo *et al.*[32] Since that time it has been clearly shown that solid-target cross sections can exceed the single-collision cross sections by an order of magnitude.[33] Further, more recent results on the same systems[34,35] suggest that the cross sections of Ref. 32 are high, arguably an effect of the target thicknesses used, a conclusion also drawn by Meyerhof *et al.*[11]

In Paper II of a recent, extensive review of K-vacancy-production mechanisms in heavy-ion–atom collisions, Meyerhof *et al.*[11] reexamined the gas-target data. Even at that time data were still sparse but were sufficient to show that neither a scaling of the (H+H) cross section[36] for symmetric systems, nor a modified-semiclassical-approximation model put forward by Briggs[37] was at all adequate.

We have also tried to scale using the $2p_{3/2}$ UA binding energy in place of the $2p_{1/2}$ UA value. For most of the collision systems, this procedure has little effect since the two levels are very nearly degenerate. However, for the very heavy UA systems (e.g., I-Xe, Br-Xe, I-Kr), where this is no longer true, the data do not appear to scale as smoothly with the UA $2p_{3/2}$ as with the $2p_{1/2}$ UA binding energy. Since $\sigma_{\rm rot}$ values deviate from the scaled values also in this region,[38] we are inclined to attach little significance to this effect.

Meyerhof *et al.*[11] also searched for a coalescence of data in the form $\sigma_K = N(v_1)\sigma_{\rm rot}$, where $\sigma_{\rm rot}$ is the $2p\pi$-$2p\sigma$ rotational coupling cross section. $N(v_1)$ would be identified with the probability of finding a vacancy in the $2p\pi_x$ MO. No simple pattern emerged and our new data do nothing to repair this situation.

Against this last failure, however, one should consider the impact-parameter dependence $P(b)$ of K-shell ionization. Cocke *et al.*[10] have concluded from particle x-ray coincidence measurements for 15- and 30-MeV Cl→Ar that $2p\pi$-$2p\sigma$ rotational coupling is operative, even in single collisions. Lutz *et al.*[12] have made impact-parameter measurements for the Ar→Ar system at 2.5, 4.5, and 8.0 MeV. Although these experimental conditions closely resemble those of Cocke *et al.*,[10] paradoxically the two sets of results appear to be incompatible. In fact, Lutz *et al.* conclude that *no* theory can presently account for the rapid increase of $P(b)$ at small b.

Annett[39] has measured the impact-parameter dependence of K x-ray emission for 50- and 65.6-MeV Cu→Ni collisions (solid targets). Their results yield a $P(b)$ curve that is similar to that expected for $2p\pi$-$2p\sigma$ rotational coupling, although the broad maximum in $P(b)$ is displaced

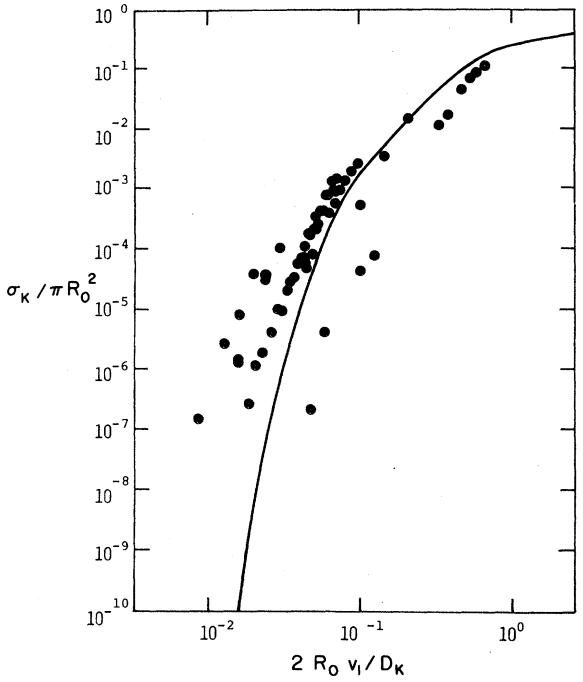

FIG. 11. K-vacancy-production cross sections from Fig. 3, but plotted using the diffusion-model parameters (see text). The abscissa is the reduced projectile velocity $w = 2R_0 v_1 / D_K$. The smooth curve is $S(w)$ from Ref. 14.

to impact parameters smaller than predicted by theory. The form of $P(b)$ is independent of the Ni-target-foil thickness ($t = 4.7$ nm and $t = 8.3$ nm), suggesting that $P(b)$ for single collisions has the same dependence on impact parameter for gaseous and foil targets (since the single-collision contribution to the total K x-ray yield will be larger for the thinner foils).

Brandt and Jones[14] have recently proposed a diffusion model, following the work of Mittleman and Wilets.[40] Although the original model was proposed to explain "single ionization" in *gas-target* collisions, Johnson *et al.*[41] and Jones *et al.*[42] have used it to describe *solid-target* impact-parameter results. In Fig. 11 we show our total cross-section gas-target data, together with the prediction, $S(w)$, of this diffusion (or statistical) model shown by the solid curve. The abscissa is $w = 2R_0 v_1 / D_K$, where $R_0 = 0.8853\, a_0 (Z_1^{2/3} + Z_2^{2/3})^{-1/2}$, a_0 being the Bohr radius, v_1 being the projectile velocity, and D_K is the diffusion constant:

$$D_K = [\tfrac{1}{20}(Z_1 + Z_2)]^3 \, (\hbar / m_e) \, .$$

The ordinate is $\sigma_K / \pi R_0^2$. The discrepancies between the experimental data and the predicted

curve are large and we conclude that the statistical model is unable to describe our single-collision cross-section results.

V. CONCLUSIONS

We have measured absolute K-ionization cross sections under single-collision conditions, for a variety of symmetric and near symmetric collision partners and over a wide energy range. Our results produce an empirical scaling law that may be used to predict (within a factor of 2) the single-collision total K-vacancy cross section for arbitrary species $Z_1 \rightarrow Z_2$, $Z_1, Z_2 \geq 16$, and so long as (i) the asymmetry condition $0.6 \lesssim Q \leq 1.0$ is fulfilled, (ii) the projectile velocity $v_1 < v_K$, and (iii) there are no $2p$ vacancies in either the projectile or target atom prior to the collision. Under these conditions

$$\sigma_K(Z_1 \rightarrow Z_2) \equiv \sigma_K(Z_2 \rightarrow Z_1) ,$$

contrary to the general result for solid targets. The effect of deliberately opening the projectile $2p$ shell through projectile stripping has been examined and an explanation offered for the observed increases in x-ray cross section.

For more asymmetric systems, $Q \approx 0.5$, markedly different cross-section systematics emerge. This is in the region of K-L level matching.

To our knowledge there is still no theory that can account satisfactorily for the symmetric *and* asymmetric cross-section magnitudes and systematics, despite the suggestive ordering of data through a scaling relationship based upon the UA $2p_{1/2}$ binding energy. Nevertheless, the total body of K-vacancy cross sections, augmented by the present data, represents a substantial challenge to any new theory of K-ionization in heavy-ion–atom collisions.

ACKNOWLEDGMENTS

We are grateful to A. Warczak, C. Annett, U. Schiebel, and R. L. Kauffman for providing us with recent single-collision data prior to publication, and to Y. Imahori for developing the heavy-ion beams from the MP tandem accelerator.

APPENDIX: ELASTIC-SCATTERING CROSS SECTIONS

In order to deduce the absolute ionization cross section from our measurements, we must know the cross section for elastic scattering of particles into a detector viewing the target at a laboratory scattering angle ϕ. Since all measurements were made with $\phi \approx 44°$, we shall use this value in the following discussion.

Lindhard *et al.*[43] have shown that the relevant parameter to consider in particle scattering $Z_1 \rightarrow Z_2$ (where $M_1 \sim M_2$) is

$$t^{1/2} = (E_{\text{c.m.}} a / Z_1 Z_2 e^2) \sin(\tfrac{1}{2}\theta) , \tag{A1}$$

where θ is the center-of-mass scattering angle, $E_{\text{c.m.}}$ is the center-of-mass-energy, and

$$a = 0.8853\, a_0 (Z_1^{2/3} + Z_2^{2/3})^{-1/2} .$$

For values of $t^{1/2} \gtrsim 10$, the scattering cross section σ_s can be described by the Rutherford formula to within 4%. We have pointed out[16] that one may safely use the Rutherford scattering cross section in near-symmetric single collisions ($Z_1 \sim Z_2$) when detecting elastically scattered particles at $\phi \sim 45°$ if the projectile energy E_1 (MeV) fulfills the requirement $E_1 \gtrsim \frac{1}{800} Z^{7/3}$, where $Z = (Z_1 Z_2)^{1/2}$.

For $Z_1 \ll Z_2$, Andersen *et al.*[44] have made measurements for ^{1}H, ^{4}He, and ^{7}Li projectiles on Au targets, $3° \leq \phi \leq 15°$. Their results indicate that the measured values of the scattering cross sections agree with those expected from the Thomas-Fermi theory when $t^{1/2} \gtrsim 2$. The same result obtains for heavy ions.[45]

Our lowest value of $t^{1/2}$ for heavy-ion scattering is for 0.4-MeV Ar → Ar, $t^{1/2} = 3.8$ (see column 3 of Table II). We used $\sigma_s = \sigma_{\text{TF}} = \sigma_{\text{Ruth}}/1.17$ for this case. Similarly, σ_{TF} has been used for all cases where $t^{1/2} < 20$; however, for most of the data, $t^{1/2} > 20$ and we may safely set $\sigma_s = \sigma_{\text{Ruth}}$. The last column of Table I (in Sec. II) shows the minimum $t^{1/2}$ values for all systems studied.

It is obvious that by assuming the form of the scattering cross section one may use the observed scattered projectile and recoil target atom relative yields to solve for the scattering angle. We have done this for different asymmetric collision pairs for which the recoil and scattered particle energies are resolved. The angle thus calculated reproduced the known geometry within 0.2°, i.e., the scattering cross sections adopted are consistent with the observed yields.

[1] J. D. Garcia, R. J. Fortner, and T. M. Kavanagh, Rev. Mod. Phys. 45, 111 (1973).
[2] U. Fano and W. Lichten, Phys. Rev. Lett. 14, 627 (1965).
[3] J. S. Briggs and J. Macek, J. Phys. B 5, 579 (1972).
[4] W. E. Meyerhof, Phys. Rev. Lett. 31, 1341 (1973).
[5] W. N. Lennard and I. V. Mitchell, J. Phys. B 9, L317 (1976).

[6]T. J. Gray, P. Richard, R. K. Gardner, K. A. Jamison, and J. M. Hall, Phys. Rev. A 14, 1333 (1976).
[7]Q. C. Kessel and B. Fastrup, Case Stud. At. Phys. 3, 137 (1973).
[8]F. W. Saris, C. Foster, A. Langenberg, and J. van Eck, J. Phys. B 7, 1494 (1974).
[9]L. Winters, M. D. Brown, L. D. Ellsworth, T. Chiao, E. W. Pettus, and J. R. Macdonald, Phys. Rev. A 11, 174 (1975).
[10]C. L. Cocke, R. R. Randall, S. L. Varghese, and B. Curnutte, Phys. Rev. A 14, 2026 (1976).
[11]W E. Meyerhof, R. Anholt, and T. K. Saylor, Phys. Rev. A 16, 169 (1977).
[12]H. O. Lutz, W. R. McMurray, R. Pretorius, R. J. van Reenen, and I. J. van Heerden, Phys. Rev. Lett. 40, 1133 (1978).
[13]C. Foster, T. P. Hoogkamer, P. Woerlee, and F. W. Saris, J. Phys. B 9, 1 (1976).
[14]W. Brandt and K. W. Jones, Phys. Lett. A 57, 35 (1976).
[15]I. V. Mitchell, W. N. Lennard, and J. S. Forster (unpublished).
[16]W. N. Lennard, I. V. Mitchell, and D. Phillips, in Seventh International Conference on Atomic Collisions in Solids, Moscow, USSR, September, 1977 (unpublished).
[17]W. Bambynek, B. Crasemann, R. W. Fink, H. U. Freund, H. Mark, C. D. Swift, R. E. Price, and P. V. Rao, Rev. Mod. Phys. 44, 716 (1972).
[18]F. C. Jundt, H. Kubo, and K. H. Purser, in *Proceedings of the International Conference on Inner Shell Ionization Phenomena and Future Applications*, edited by R. W. Fink *et al.* (USAEC, Oak Ridge, Tenn., 1973), p. 1450.
[19]W. N. Lennard and I. V. Mitchell, Nucl. Instrum. Methods 132, 39 (1976).
[20]R. Anholt, Phys. Rev. A 17, 834 (1978).
[21]W. E. Meyerhof, R. Anholt, T. K. Saylor, S. M. Lazarus, A. Little, and L. F. Chase, Jr., Phys. Rev. A 14, 1653 (1976).
[22]W. E. Meyerhof, R. Anholt, J. Eichler, and A. Salop, Phys. Rev. A 17, 108 (1978).
[23]B. Fricke and G. Soff, At. Data Nucl. Data Tables 19, 83 (1977).
[24]J. A. Bearden, Rev. Mod. Phys. 39, 78 (1967).
[25]R. Schuch, G. Nolte, W. Lichtenberg, H. Schmidt-Böcking, R. Schulé, and I. Tserruya, Z. Phys. A 284, 153 (1978).
[26]W. N. Lennard, I. V. Mitchell, J. S. Forster, and D. Phillips, J. Phys. B 10, 2199 (1977).
[27]U. Schiebel, B. L. Doyle, and L. D. Ellsworth, Bull. Am. Phys. Soc. 22, 656 (1977); Z. Phys. A 285, 241 (1978).
[28]A. Warczak, D. Liesen, J. R. Macdonald, and P. H. Mokler, Z. Phys. A 285, 235 (1978).
[29]R. J. Fortner, P. H. Woerlee, S. Doorn, T. P. Hoogkamer, and F. W. Saris, Phys. Rev. Lett. 39, 1322 (1977).
[30]W. E. Meyerhof, R. Anholt, T. K. Saylor, and P. D. Bond, Phys. Rev. A 11, 1083 (1975).
[31]J. S. Hansen, Phys. Rev. A 8, 822 (1973).
[32]H. Kubo, F. C. Jundt, and K. H. Purser, Phys. Rev. Lett. 31, 674 (1973).
[33]I. V. Mitchell, W. N. Lennard, J. S. Forster, and F. W. Saris, in *Electronic and Atomic Collisions, Abstracts of X ICPEAC* edited by M. Barat and J. Reinhardt (Paris, 1977), Vol. 1, p. 324.
[34]J. S. Greenberg, P. Vincent, and W. Lichten, Phys. Rev. A 16, 964 (1977).
[35]R. Laubert, H. Haselton, J. R. Mowat, R. S. Peterson, and I. A. Sellin, Phys. Rev. A 11, 135 (1975).
[36]V. SethuRaman, W. R. Thorson, and C. F. Lebeda, Phys. Rev. A 8, 1316 (1973).
[37]J. S. Briggs, J. Phys. B 8, L485 (1975).
[38]R. Anholt, W. E. Meyerhof, and A. Salin, Phys. Rev. A 16, 951 (1977).
[39]C. H. Annett, Master's thesis (Kansas State University, 1977) (unpublished).
[40]M. H. Mittleman and L. Wilets, Phys. Rev. 154, 12 (1967).
[41]B. M. Johnson, K. W. Jones, and D. J. Pisano, Phys. Lett. A 59, 21 (1976).
[42]K. W. Jones, H. W. Kraner, and W. Brandt, Phys. Lett. A 57, 33 (1976).
[43]J. Lindhard, V. Nielsen and M. Scharff, K. Dan. Vidensk. Selsk. Mat.-Fys. Medd. 36, No. 10 (1968).
[44]H. H. Andersen, J. Bøttiger, and H. Knudsen, Phys. Rev. A 7, 154 (1973).
[45]H. Knudsen and P. Møller Petersen, J. Phys. B 11, 455 (1978).
[46]A. Langenberg and J. van Eck, J. Phys. B 9, 2421 (1976).
[47]W. N. Lennard and I. V. Mitchell, Phys. Rev. A 12, 1723 (1975).
[48]C. Stoller, Laboratorium für Kernphysik, Annual Report, ETH Zürich (1976) (unpublished); and private communication.
[49]G. Basbas, W. Brandt, and R. Laubert, Phys. Rev. A 7, 983 (1973).
[50]E. M. Middlesworth, Jr., D. J. Donahue, L. C. McIntyre, Jr., and E. M. Bernstein, Phys. Rev. A 17, 141 (1978).
[51]R. L. Kauffman and L. C. Feldman, Bull. Am. Phys. Soc. 22, 654 (1977); and private communication.
[52]L. M. Winters, J. R. Macdonald, M. D. Brown, L. D. Ellsworth, and T. Chiao, Phys. Rev. A 7, 1276 (1973).